



## Application of response surface methodology to optimize 4-nitrophenol adsorption by prepared molecular imprinting polymers

Yiqi Liu<sup>a</sup>, Gang Xue<sup>a</sup>, Yaqian Ma<sup>a</sup>, Lei Ding<sup>a,b,\*</sup>, Yanli Kong<sup>a,b,\*</sup>, Yang Gao<sup>a</sup>, Zhonglin Chen<sup>c,d</sup>

<sup>a</sup>School of Civil Engineering and Architecture, Anhui University of Technology, Maanshan, Anhui, 243002, China, emails: dllyan@ahut.edu.cn (L. Ding), kyl0821@ahut.edu.cn (Y.L. Kong), lyq3618199@126.com (Y.Q. Liu), xuegang5288@163.com (G. Xue), 2912194852@qq.com (Y.Q. Ma), 546167328@qq.com (Y. Gao)

<sup>b</sup>Engineering Research Center of Biomembrane Water Purification and Utilization Technology, Ministry of Education, Maanshan, Anhui, 243002, China

<sup>c</sup>State Key Laboratory of Urban Water Resources and Environment, School of Municipal & Environmental Engineering, Harbin Institute of Technology, Harbin 150090, China, email: zhonglinchen@hit.edu.cn (Z.L. Chen)

<sup>d</sup>HIT Yixing Academy of Environmental Protection, Yixing 214200, China

Received 10 March 2022; Accepted 17 November 2022

### ABSTRACT

4-Nitrophenol (4-NP) removal using prepared molecular imprinting polymers (MIPs) as a specific adsorbent was investigated. On the basis of single-factor experiment, Box–Behnken statistical experiment design (BBD) and response surface methodology (RSM) were used to investigate the influence of MIPs dosage, initial concentration of 4-NP, pH and temperature of the solution, and their potential interaction effect on 4-NP removal. The quadratic polynomial regression model of response value  $Y$  (4-NP removal efficiency) was established based on the BBD experimental results. The reasonable and reliable of regressive of the model was confirmed by the analysis of variance test and residuals analysis ( $R^2 = 0.9952$ ). The RSM model indicates that all single-factors had a significant effect on 4-NP removal. The interaction effect between MIPs dosage and temperature, temperature, and pH were not significant but the other four interaction effects were significant. The regression model showed an optimum removal of 79.63%, while 78.39% removal was obtained from batch experiments at the optimum conditions suggested by the regression model, which reconfirmed the validity of the model. The results demonstrated that prepared MIPs possessed a strong adsorption ability for 4-NP removal, allowing a possible practical application in future water treatment.

**Keywords:** 4-nitrophenol; Molecular imprinting; Adsorption; Response surface methodology

### 1. Introduction

4-nitrophenol (4-NP) is one of the most important chemical materials, and a typical organic pollutant present in the environment [1]. Pesticides, medicine, dyes, and petroleum are the major industrial processes leading to anthropogenic 4-NP contamination [2]. The remained 4-NP in water bodies can contaminate surface and/or groundwater sources due

to its strong toxicity, high water solubility, and not easy to be degraded properties [3]. 4-NP exposure can cause great harm to human beings even at a low concentration condition and notice that it should be paying more attention to its long-term toxicity and comprehensive impact on the ecological environment [4]. Therefore, the exploration of technologies for the treatment of potable water and industrial wastewater containing 4-NP is an urgent priority for many countries.

\* Corresponding authors.

Various technologies are available for the removal of 4-NP from contaminated water including oxidation [5], membrane separation [6], microorganism [7], etc. Adsorption is cost-effective for large flow rates and its advantages of simple operation and high efficiency. At present, there has been a large number of studies on 4-NP removal in wastewater [8]. However, a systematic study on the removal of 4-NP in the environment and potable water is currently lacking. Considering that 4-NP was at a relatively low concentration in the environmental water, in addition, other impurities might have serious negative impacts on 4-NP removal, it is necessary to explore an efficient selective adsorbent for the 4-NP removal in the water source.

Molecular Imprinting Technology (MIT) has become an emerging technology based on the “antigen-antibody” theory in recent years [9]. The principle of molecular imprinting polymers (MIPs) is to select specific substances as template molecules and synthesize corresponding imprinted molecular polymers [10]. After the template molecules are eluted, the imprinted materials with selective adsorption ability can be obtained, and the performance of specific detection or removal of object pollutant and its analogues can be achieved. Moreover, the prepared molecular imprinting materials are of great economical to recycle adsorbed, and eluted by good mechanical and reproducibility [11].

The methods of synthesizing MIPs include bulk polymerization [12], precipitation polymerization [13], emulsion polymerization [14], suspension polymerization [15], and surface imprinting [16]. Surface imprinting has been developed as a new method for preparing imprinted polymers with numerous merits, such as rich imprinting points, faster recognition speed, and simple preparation processes [17]. Di Bello et al. [18] proposed synthesizing a chitosan based molecularly imprinted technology for the detection and quantification of 4-nitrophenol in aqueous media. An et al. [19] synthesized a series of surface molecularly imprinted polymers using 2-nitrophenol, 3-nitrophenol, 4-nitrophenol, and 4-methylphenol as template, respectively. Liang et al. [20] synthesized  $\text{Fe}_3\text{O}_4@\text{SiO}_2@\text{PNP-SMIP}$  surface imprinted polymer and the adsorption capacity of this polymer for 4-NP can reach 134.23 mg/g.

As the Surface Molecular Imprinting Technology (SMIT) gradually develops and matures, more preparation methods for surface molecularly imprinted materials have emerged. The common preparation methods are: sacrificial carrier [21], solid-phase synthesis [22], electro polymerization [23], chemical grafting [24] and sol-gel method [25].

The sol-gel method was proposed as a simple, relatively low-cost methodology providing products of high thermal and mechanical stability as solid phases for applications in various areas of research [26]. SMIT combined with the sol-gel technique, which is characterized by the complete removal of templates, high binding capacity and selectivity, faster mass transfer, and easy preparation [27].

Currently, preparation technology by using surface imprinting and sol-gel method has been broadly applied in water treatment. Hao et al. [28] synthesized a fluorescent material by coating an imprinted polymer layer on the surface of C-dots by a sol-gel process, which was used for selective recognition and fluorescence detection of the target molecule 4-NP. Guo et al. [27] prepared

a dual-dummy-template molecular imprinted material by using the sol-gel imprinting method on the surface of magnetic graphene oxide (MGO) modified with mesoporous silica ( $\text{mSiO}_2$ ). The prepared MIPs revealed a high adsorption capacity for phthalates esters (PAEs). Raof et al. [29] synthesized a molecularly imprinted silica gel sorbent (2-HA-MISG) for selective removal of 2-hydroxybenzoic acid (2-HA) was prepared by a surface imprinting technique with a sol-gel process. 2-HA-MISG displayed fast uptake kinetics (within 20 min) and high adsorption capacity (76.2 mg/g).

However, the research on a new surface molecular imprinting material for selective adsorption of 4-NP pollutants removal is inadequate. Therefore, our research team successfully prepared a novel imprinted material (MIPs) for 4-NP removal and noted that MIPs could be possibly used as adsorbent to remove 4-NP from raw water through a systematic comparative study [30]. However, the adsorption process has not been optimized. Moreover, the interactions between parameters affecting the removal of 4-NP by MIPs have not been investigated yet.

In the present study, the Box-Behnken (BBD) design and response surface methodology (RSM) were selected to optimize major operating variables for optimization of process variables which influence the removal efficiency of contaminations. It is an effective method to optimize process conditions and it can determine the influence of various factors and their interactions on the indexes under investigation (response value) during technological operations [31].

RSM is widely used in various fields, for example, the influence of ultrasound-assisted magnetic adsorption system characteristics on 2,4-dinitrophenol adsorption [32], optimization of degradation of dimethyl phthalate using persulfate activated by UV and ferrous ions [33], optimization of sulfate removal from wastewater using magnetic multi-walled carbon nanotubes [34], optimization of chromium biosorption by orange peels [35].

By studying the RSM, a particular set of mathematical and statistical methods, the experiments can be designed and a suitable model can be established. More delightfully, levels of the independent variables can be evaluated

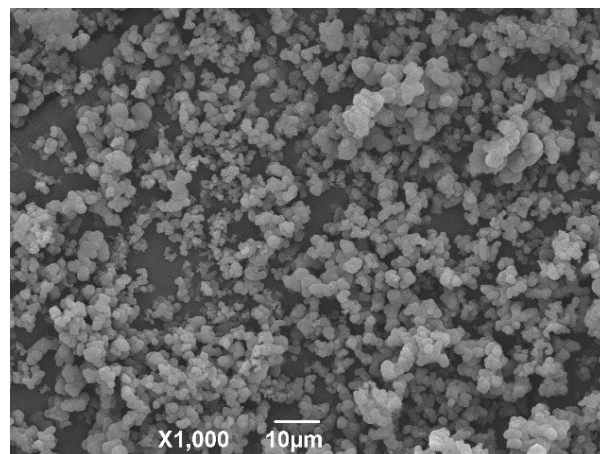


Fig. 1. Scanning electron microscopy images of MIPs.

through RSM involves statistical design of experiments based on the multivariate non-linear model.

Therefore, the main objectives of this study are to optimize the process parameters influencing the removal of 4-NP adsorbed on MIPs, a new type prepared by the surface Molecular Imprinting Technology coupled with the sol-gel method. In this study, the BBD design in RSM was applied to investigate the effect of important operating parameters on the removal rate of 4-NP and to find the most appropriate combination of variables to maximize the removal efficiency of 4-NP. The findings provided new insight into the availability of BBD for 4-NP removal by a novel prepared MIPs adsorbent and better understanding the relationship among the independent variables and the response on 4-NP removal efficiency.

## 2. Materials and methods

### 2.1. Materials

4-nitrophenol (4-NP,  $C_6H_5NO_3$ ),  $\alpha$ -methacrylic acid ( $\alpha$ -MAA,  $C_4H_6O_2$ ), hydrochloric acid (HCl), sodium hydroxide (NaOH), and methanol ( $CH_3OH$ ) were purchased from Sinopharm Chemical Reagent Co., Ltd., (Beijing, China). Trimethylolpropane trimethacrylate (TRIM,  $C_{18}H_{26}O_6$ ) was purchased from Aladdin Reagent Co., Ltd., (Shanghai, China). Azobisisobutyronitrile (AIBN,  $C_8H_{12}N_4$ ) was purchased from Tianjin Guangfu Fine Chemical Research Institute (Tianjin, China). Ethanol ( $CH_3CH_2OH$ ) was purchased from Shanghai Zhenya Chemical Reagent Co., Ltd., (Shanghai, China). Acetic acid ( $CH_3COOH$ ) was purchased from Shanghai Lingfeng Chemical Reagent Co., Ltd., (Shanghai, China). All chemicals were of analytical grade and used as received without further purification. Deionized water was used as the solvent throughout the experiments.

### 2.2. Methods

#### 2.2.1. Preparation and characterization of MIPs

Our previous research [30] had successfully prepared the MIPs with the optimum 4-NP removal effect of 77.87%. MIPs was prepared with 4-NP as template molecule,  $\alpha$ -MAA as functional monomer, TRIM as crosslinking agent, and AIBN as initiator. The molar ratio of 4-NP to  $\alpha$ -MAA and TRIM was 1:8:10, and the pore formation agent was ethanol. In addition, the extracting solution was methanol/acetic acid with a volume ratio of 7:3. The MIPs prepared under the optimal process conditions were characterized (Fig. 1). These characterization analyses have shown that MIPs was irregular spherical particle with an average pore diameter of 3.74 nm, and the rough surface of each spherical particle was cross-linked to form more porous holes' surface, reaching a specific surface area of 183.32  $m^2/g$ . Moreover, Fourier-transform infrared spectroscopy results showed that 4-NP molecular imprinting was successfully imprinted in the functional monomer polymerized under the action of the crosslinking agent. Furthermore, the surface of MIPs was acidic with the zero-point potential  $pH_{pzc}$  of the prepared imprinting material 2.27. Therefore, it is necessary to investigate and adjust optimal removal conditions which would be more conducive to 4-NP removal by MIPs.

#### 2.2.2. 4-NP analytical methods

Quantification of 4-NP concentration was performed on an Agilent 1260 HPLC. Separation was carried out using a 4.6 mm  $\times$  250 mm Acclaim TM C18 column (Thermo, USA). The instrumental conditions were as follows: the mobile phase is methanol/water (V/V = 6:4) with a flow rate of 1 mL/min at the temperature of 303 K. The injection quantity is 10  $\mu$ L at the detection wavelength of 228 nm.

#### 2.2.3. Batch adsorption experiments

Batch adsorption experiments were performed in the shaking flask experiment, 10  $\mu$ mol/L of 4-NP solution (40 mL) was added to the conical flask, and then a certain amount of prepared MIPs was added to the conical flask, immediately mixed with a constant agitation speed of 150 rpm for 180 min at 303 K water bath constant temperature.

Subsequently, the experiments were carried out at different initial 4-NP concentrations, solution pH, MIPs dosage, and solution temperature. Sampling was conducted at desired time intervals, and MIPs was separated from the solution by using a 0.45  $\mu$ m Millipore membrane filter. After filtration, the 4-NP in filtrate was determined. Each experiment was carried out in (at least) duplicate. The adsorption capacity and removal rate of 4-NP were evaluated by Eqs. (1) and (2):

$$q_t = \frac{(C_0 - C_t)V}{W} \quad (1)$$

$$E = \frac{(C_0 - C_t)}{C_0} \times 100\% \quad (2)$$

where  $q_t$  is the saturated adsorption capacity ( $\mu$ mol/g),  $C_0$  and  $C_t$  are 4-NP concentration of 0 min and  $t$  min ( $\mu$ mol/L),  $V$  is the volume of solution (L),  $W$  is the amount of adsorbent (g), and  $E$  is the removal rate (%).

#### 2.2.4. Response surface experiment

The RSM experiments were designed by Design-Expert 8.0 software (State-Ease Inc., Minneapolis, USA) based on the BBD model. According to the design principle of BBD model, 29 groups of response surface tests are designed. The level of various independent variables at coded values of response surface methodology experimental design was shown in Table 1. The optimization of 4-NP uptake was carried out by four chosen independent process variables and 4-NP removal efficiency was the response ( $Y$ ) (dependent variable), initial 4-NP concentration ( $X_1$ ) was varied between 10 and 50  $\mu$ mol/L, MIPs dosage ( $X_2$ ) was ranged from 1.0 to 1.5 g/L, and solution temperature ( $X_3$ ) was varied between 293 and 313 K, while pH value ( $X_4$ ) was ranged from 4 to 8. The low, middle and high levels of each variable were designated as -1, 0, and +1, respectively. An empirical second-order polynomial model ( $Y$ ) (response function) for predicting the optimal point was in Eq. (3):

$$Y_{\text{predicted}} = \beta_0 + \sum \beta_i x_i + \sum \beta_{ii} x_i^2 + \sum \beta_{ij} x_i x_j + \varepsilon \quad (3)$$

where  $Y$  is the predicted value,  $\beta_0$  is the constant coefficient,  $\beta_r$ ,  $\beta_{ii}$  and  $\beta_{ij}$  are the regression coefficients of the linear, quadratic and interactive effect regression coefficient between the input variables,  $x_i$  and  $x_j$  are the input variables,  $\varepsilon$  is the measurement error. The validity of the model and the reliability of the statistical experimental strategies were determined by comparing the experimental and predicted values. The reliability of the established regression model is verified by various methods. Furthermore, the interaction of influential variables on the removal rate of 4-NP was evaluated in an additional study.

### 3. Results and discussion

#### 3.1. Adsorption properties of MIPs for removal of 4-NP

The removal of 4-NP by MIPs as functions of solution pH, initial 4-NP concentration, adsorbent dosage, and solution temperature are shown in Fig. 2. As illustrated in

Fig. 2a, the adsorption capacity of MIPs for 4-NP removal decreased as pH increased. At pH 2–4, the amount of 4-NP removed increased significantly with a maximum adsorption capacity is 6.23  $\mu\text{mol/g}$  and a maximum removal rate of 77.84%. However, many different phenomena were observed under alkaline conditions, 4-NP removal experienced a gradual drop, which should be ascribed to the electrostatic repulsion with negatively charged MIPs. Fig. 2b reveals that the adsorption capacity of MIPs for 4-NP removal increased with the increase of initial concentration. When the initial concentration increases, the number of MIPs active sites does not increase correspondingly. However, the active sites of MIPs would be well occupied in this situation as more 4-NP would be in the vicinity of MIPs. As a result, the absolute amount of 4-NP that is removed increased. As demonstrated in Fig. 2c, the removal of 4-NP by MIPs generally increased with the increasing MIPs dosage, from 21.77% to 86.25% as MIPs dosages increased from 1.0 to 1.5 g/L. This is due to the accompanied increase of total surface area and reaction sites. Fig. 2d shows that the adsorption capacity of MIPs can be divided into two stages at all temperature levels examined in this study. 4-NP removal increased gradually with increasing temperature and then experienced a gradual drop. High temperature can lead to a rise of 4-NP mobility from the bulk solution toward the surface of MIPs, consequently promoting activation [36]. Moreover, the pore structure of MIPs might become larger due to thermal expansion and contraction, reducing the mass transfer resistance of 4-NP in the imprinted material [37]. However, excessive temperature might result in the violent diffusion of 4-NP molecules in the solution, leading to the destruction of

Table 1  
Selected factors and levels of RSM experiments

Code	Factors	Variable level and range		
		-1	0	1
A	Initial 4-NP concentration ( $\mu\text{mol/L}$ )	10	30	50
B	MIPs dosage (g/L)	1	1.25	1.5
C	Temperature (K)	293	303	313
D	Solution pH	4	6	8

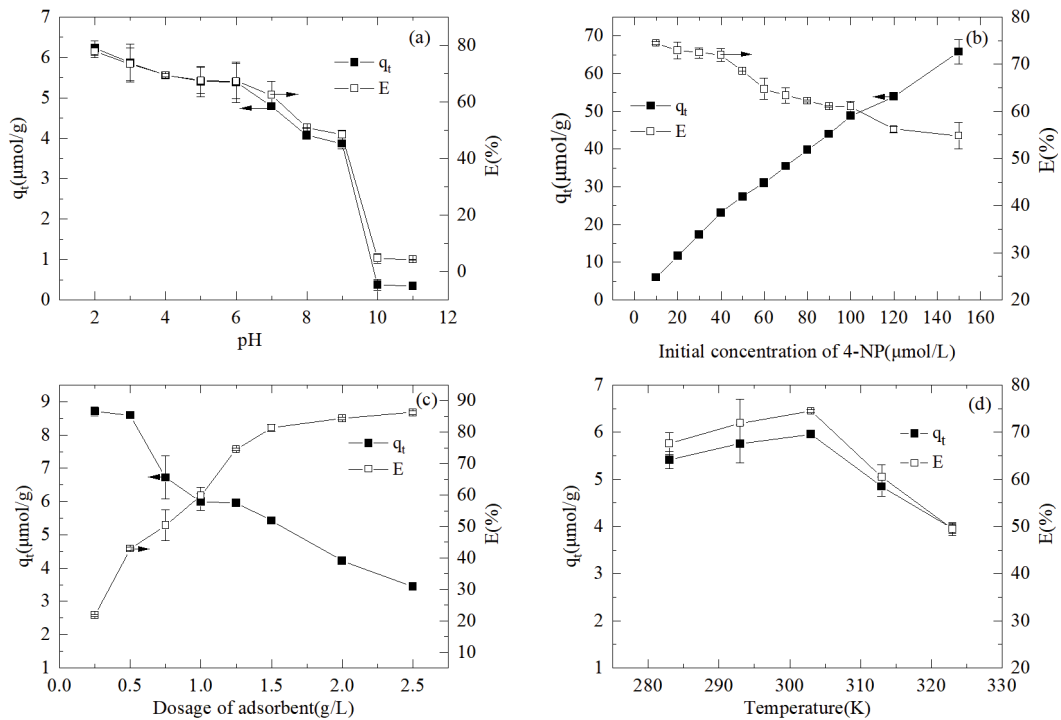


Fig. 2. (a) Influence of pH on the removal of 4-NP, (b) influence of initial concentration on the removal of 4-NP, (c) influence of adsorbent dosage on the removal of 4-NP, and (d) influence of temperature on the removal of 4-NP.

hydrogen bonds and covalent bonds formed between the template molecule and the binding site, reducing the removal rate of the target pollutants by the imprinted material.

### 3.2. RSM and BBD analysis

#### 3.2.1. Establishment of regression model equation

The experimental design and corresponding results are shown in Table 2. By fitting the experimental results, the quadratic multinomial regression model equation of the removal of 4-NP by MIPs was established. The equation is as follows:

$$Y = 63.91 + 5.16A + 4.82B - 8.46C - 11.00D - 4.66AB + 7.40AC - 4.99AD - 0.67BC + 1.97BD + 1.31CD - 0.95A^2 - 5.83B^2 - 9.48C^2 - 13.86D^2 \quad (4)$$

where  $Y$  is the response value predicted of 4-NP removal rate, and  $A$ ,  $B$ ,  $C$ , and  $D$  represent the code value of the initial 4-NP concentration, MIPs dosage, solution temperature, and solution pH value of the variables, respectively.

#### 3.2.2. Reliability analysis of regression model equation

The statistical significance of the response function was checked by analysis of variance (ANOVA), and the ANOVA results for response surface quadratic model and model terms are summarized in Table 3. The  $F$ -value and  $P$ -value are used for statistical significance of the model. The larger the  $F$ -value and the smaller the  $P$ -value indicated the more significant of the model [38]. If the  $P$ -value is not greater than 0.05, the factor is influential, and the 95% probability of the model term is significant [39]. In this study, the model  $F$ -value is 215.77 and the  $P$ -value is less than 0.0001, implying only a 0.01% chance that the model  $F$ -value this large could occur because of noise, which indicated that the model established is highly significant [40]. The  $F$ -value

Table 2  
Response surface experiment design and results

Run	4-NP concentration	MIPs dosage	Temperature	pH	Removal rate (%)	
	$A$ ( $\mu\text{mol/L}$ )	$B$ (g/L)	$C$ (K)	$D$	Experimental	Predicted
1	-1 (10)	-1 (1)	0 (303)	0 (6)	51.51	52.80
2	0 (30)	0 (1.25)	-1 (293)	-1 (4)	50.45	51.81
3	0 (30)	0 (1.25)	0 (303)	0 (6)	72.87	71.77
4	0 (30)	1 (1.5)	-1 (293)	0 (6)	53.16	52.12
5	-1 (10)	0 (1.25)	1 (313)	0 (6)	61.92	61.34
6	-1 (10)	1 (1.5)	0 (303)	0 (6)	41.27	41.80
7	0 (30)	0 (1.25)	0 (303)	0 (6)	37.00	36.73
8	0 (30)	-1 (1)	1 (313)	0 (6)	21.60	22.44
9	0 (30)	0 (1.25)	0 (303)	0 (6)	60.86	60.26
10	0 (30)	-1 (1)	-1 (293)	0 (6)	60.77	59.93
11	1 (50)	0 (1.25)	-1 (293)	0 (6)	49.17	48.26
12	0 (30)	0 (1.25)	0 (303)	0 (6)	29.10	27.95
13	0 (30)	-1 (1)	0 (303)	-1 (4)	52.78	51.58
14	0 (30)	-1 (1)	0 (303)	1 (8)	62.76	62.55
15	0 (30)	0 (1.25)	-1 (293)	1 (8)	37.54	36.00
16	-1 (10)	0 (1.25)	0 (303)	-1 (4)	44.85	44.30
17	1 (50)	0 (1.25)	0 (303)	1 (8)	73.45	74.50
18	0 (30)	1 (1.5)	1 (313)	0 (6)	48.16	49.38
19	1 (50)	1 (1.5)	0 (303)	0 (6)	42.51	42.78
20	0 (30)	0 (1.25)	0 (303)	0 (6)	46.82	47.27
21	0 (30)	0 (1.25)	1 (313)	-1 (4)	52.33	52.37
22	0 (30)	1 (1.5)	0 (303)	-1 (4)	56.62	58.07
23	1 (50)	0 (1.25)	0 (303)	-1 (4)	26.39	26.44
24	-1 (10)	0 (1.25)	0 (303)	1 (8)	38.57	40.02
25	0 (30)	1 (1.5)	0 (303)	1 (8)	64.60	63.91
26	0 (30)	0 (1.25)	1 (313)	1 (8)	63.26	63.91
27	1 (50)	-1 (1)	0 (303)	0 (6)	64.42	63.91
28	1 (50)	0 (1.25)	1 (313)	0 (6)	63.91	63.91
29	-1 (10)	0 (1.25)	-1 (293)	0 (6)	63.36	63.91

Table 3  
ANOVA for the predicted model for 4-NP removal

Source	Sum of square	Degree of freedom	Mean square	F-value	P-value	Significance
Model	4,995.29	14	356.81	215.77	<0.0001	√
A-4-NP concentration	319.47	1	319.47	193.19	<0.0001	√
B-MIPs dosage	278.79	1	278.79	168.59	<0.0001	√
C-Temperature	858.24	1	858.24	518.99	<0.0001	√
D-pH	1,450.68	1	1,450.68	877.26	<0.0001	√
AB	87.02	1	87.02	52.62	<0.0001	√
AC	219.09	1	219.09	132.49	<0.0001	√
AD	99.77	1	99.77	60.33	<0.0001	√
BC	1.78	1	1.78	1.08	0.3168	
BD	15.55	1	15.55	9.40	0.0084	√
CD	6.89	1	6.89	4.17	0.0605	
A <sup>2</sup>	5.91	1	5.91	3.57	0.0796	
B <sup>2</sup>	220.4	1	220.40	133.28	<0.0001	√
C <sup>2</sup>	582.37	1	582.37	352.17	<0.0001	√
D <sup>2</sup>	1,245.74	1	1,245.74	753.32	<0.0001	√
Residual	23.15	14	1.65	–	–	–
Lack of fit	21.68	10	2.17	5.89	0.0511	
Pure error	1.47	4	0.37	–	–	–
Correlation total	5,018.44	28	–	–	–	–
R <sup>2</sup> = 0.9954		Adequate precision = 56.291				

of the Lack of fit is 5.89 and the *P*-value is 0.0511, indicating that lack of fit was not significant. This means that the errors of the model can be ignored and the model is credible [41]. The determination coefficient (*R*<sup>2</sup>) can be used to judge the matching degree of the quadratic polynomial. The determination coefficient *R*<sup>2</sup> value of this model is 0.9954, and the predicted *R*<sup>2</sup> of 0.9747 is in reasonable agreement with the Adjusted *R*<sup>2</sup> of 0.9908, which indicates that the regression equation fits well. Adequacy precision measures the signal to noise ratio. A ratio greater than 4 is desirable. The adequacy precision of the model is 56.291, that is, the precision that can be measured is greater than 4, which indicates that the model design space of the model is reasonable. This means the model can be used to navigate the design space, analyze and predict the removal of 4-NP by MIPs. In this case, the interaction between the concentration of 4-NP and MIPs dosage (*AB*), the concentration of 4-NP and the solution temperature (*AC*), the concentration of 4-NP and the pH of the solution (*AD*), and the MIPs dosage and the pH (*BD*) have significant effects on the adsorption of 4-NP. However, the interaction between 4-NP concentration and temperature (*BC*), the temperature and pH (*CD*) have no significant effect on the adsorption of 4-NP.

Moreover, the fitting of the experimental and predicted values of the 4-NP removal rate is shown in Fig. 3. As can be seen, the model predictions fit satisfactorily with the experimental observations. Most of the data points are approximately evenly distributed on both sides of a linear line with a correlation coefficient *R*<sup>2</sup> = 0.9952, which further illustrates that the form of the model chosen to explain the relationship between the factors and the response is correct and can be used to navigate the design the removal

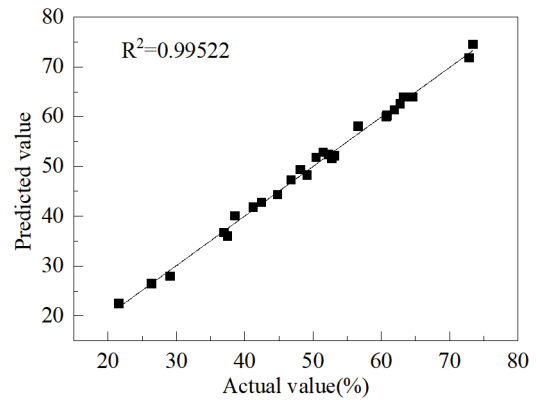


Fig. 3. Fitting graph of actual value and predicted value with respect to 4-NP removal rate.

of 4-NP by MIPs. Analysis of the residual error can also verify the reliability of the regression model established in this research. The internally studentized residuals and normal probability plot for 4-NP adsorption is shown in Fig. 4a. The internal residual data points of the model are normally distributed, which is consistent with the assumption of analysis of variance. If the predicted value is evenly distributed within the ±3 interval of the residual value, it means that the predicted value obtained by the model is accurate and reliable. As illustrated in Fig. 4b, the predicted values of the model are distributed within the confidence interval, and there are no predicted values outside the interval range, indicating that the 4-NP removal rate obtained by the regression model is accurate.

### 3.2.3. Response surface estimation for maximum removal of 4-NP by MIPs

RSM was used and results are shown in the form of 3D plots and contours as seen in Fig. 5. The combined effect of the amount of adsorbent and concentration of 4-NP on sorption is given in Fig. 5 while the other variables were

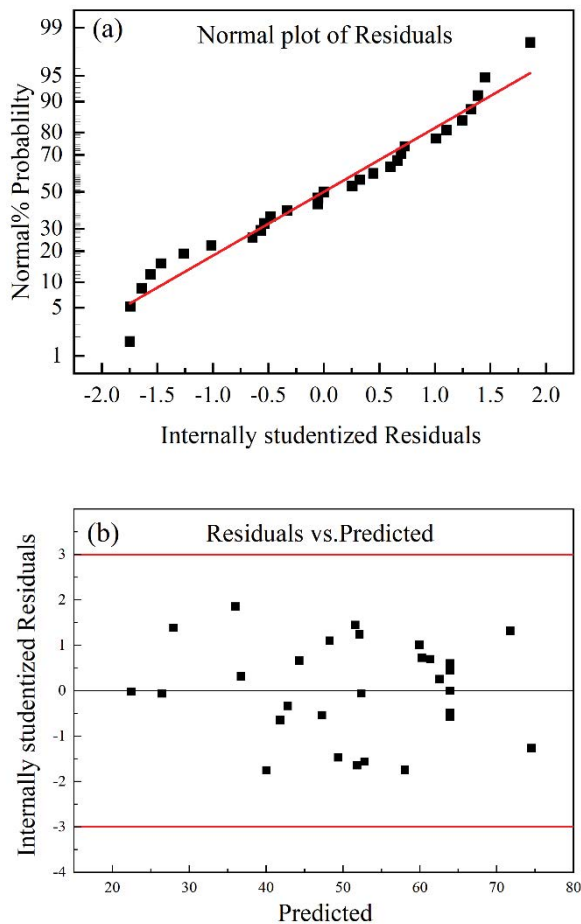


Fig. 4. (a) The internally studentized residuals and normal probability plot for 4-NP adsorption and (b) internally studentized residuals and predicted value plot for 4-NP adsorption.

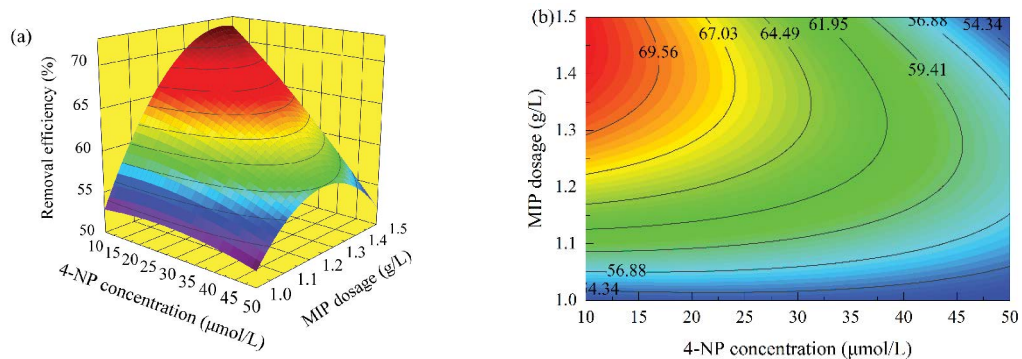


Fig. 5. (a) The 3D plot of the effect of initial 4-NP concentration and MIPs dosage on the adsorption of 4-NP and (b) contour plot of the effect of initial 4-NP concentration and MIPs dosage on the adsorption of 4-NP.

maintained constant at the statistically optimized conditions (pH = 6, temperature = 303 K). Fig. 5a shows a combination of smaller 4-NP concentration and higher MIPs dosage can enhance the 4-NP removal. The interaction between the initial 4-NP concentration and MIPs dosage (AB) has a significant effect on 4-NP removal rate. The effect of MIPs dosage on 4-NP removal rate is higher than that of the initial 4-NP concentration as demonstrated in Fig. 5b. The higher removal rate is due to much more active sites are available for 4-NP adsorption as its concentration is low. However, the limited active imprinting sites on the surface of the imprinted material with a low dosage cannot satisfy the gradual increasing of 4-NP in the solution, resulting in a reduced removal rate.

Fig. 6 reveals that the combination of 4-NP concentration and temperature on the removal of 4-NP under the condition of 1.25 g/L MIPs and pH of 6. It was observed that percentage removal of 4-NP decreased with increasing initial concentration of 4-NP at a constant reaction temperature while the effect of temperature on the 4-NP removal experienced a parabolic trend at a constant initial concentration of 4-NP. The interaction between the two has a significant impact on the 4-NP removal rate. The temperature on the 4-NP removal is more intensive in the contour map, indicating that the temperature has a higher effect on the 4-NP removal rate than the initial 4-NP concentration.

The joint effect of the 4-NP concentration and pH for 1.25 g/L MIPs at 303K is shown in Fig. 7. The removal rate of 4-NP presented a trend, first increasing and then decreasing with the increase of pH while decreasing with the increase of 4-NP concentration. The acid-base dissociation constant (pKa) of 4-NP was 7.15 [42]. 4-NP exists in molecular form under acidic conditions. The surface functional groups of MIPs are positively charged due to protonation, resulting electrostatic attraction with chloride ions which were added hydrochloric acid to adjust the pH value. In the meanwhile, phenolic compounds easily form hydrogen bonds, that is, 4-NP easily forms hydrogen bonds between MIPs, leading to the reduce the inhibitory effect of chloride ions. When the pH is greater than 7, 4-NP exists in the form of anion. There is electrostatic repulsion between MIPs and 4-NP. The hydroxyl ions in the solution will compete with 4-NP for adsorption, reducing the removal rate of 4-NP. The contour map shows that the effect of pH on the removal rate of

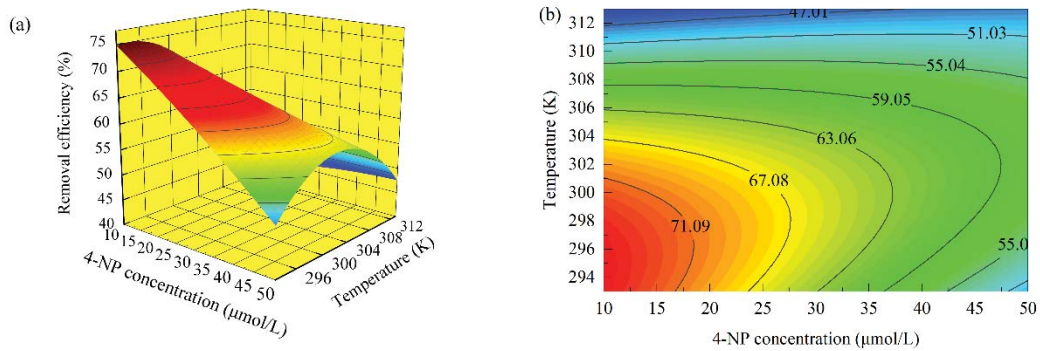


Fig. 6. (a) The 3D plot of the effect of initial 4-NP concentration and temperature on the adsorption of 4-NP and (b) contour plot of the effect of initial 4-NP concentration and temperature on the adsorption of 4-NP.

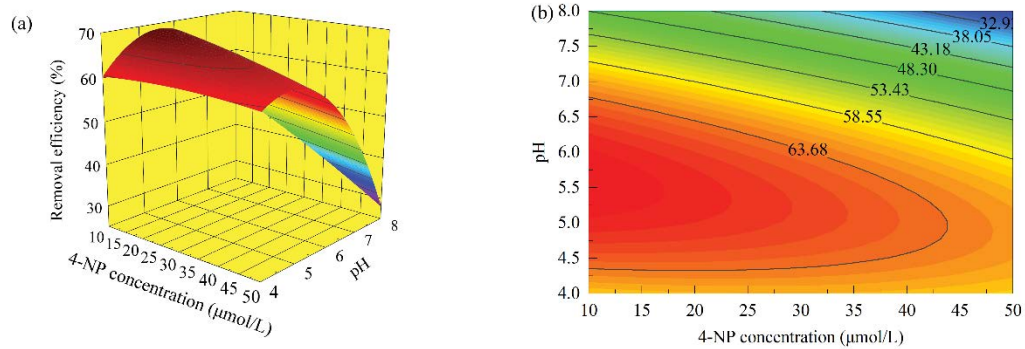


Fig. 7. (a) The 3D plot of the effect of initial 4-NP concentration and pH on the adsorption of 4-NP and (b) contour plot of the effect of initial 4-NP concentration and pH on the adsorption of 4-NP.

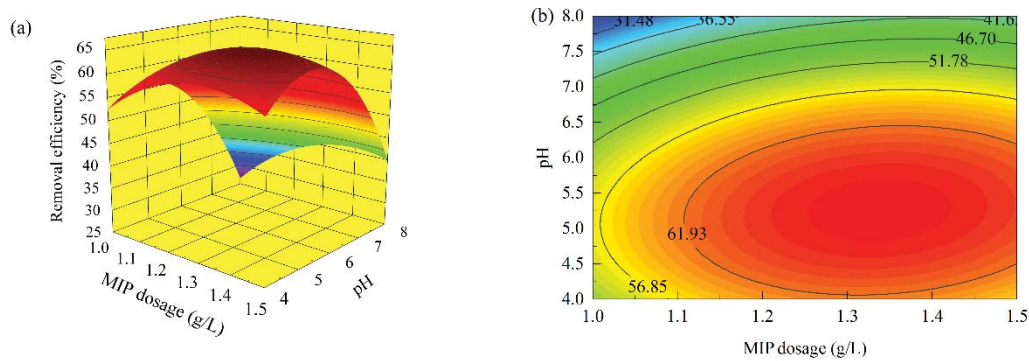


Fig. 8. (a) The 3D plot of the effect of MIPs dosage and pH on the adsorption of 4-NP and (b) contour plot of the effect of MIPs dosage and pH on the adsorption of 4-NP.

4-NP is higher than that of the initial 4-NP concentration. The optimal point of the model effect is pH 5–6 and the initial concentration of 4-NP is 10–30  $\mu\text{mol/L}$ .

The interaction of MIPs dosage and pH on the removal of 4-NP is shown in Fig. 8 under the condition of 4-NP concentration of 30  $\mu\text{mol/L}$  and 303 K. The removal of 4-NP first increased and then decreases with increasing in pH and MIPs dosage. The pH may change the degree of ionization of the functional monomer, the form, and electronegativity of the template molecule, and will affect the adsorption

process. In this study, increasing of pH resulted in the trend of the parabola in the removal rate of 4-NP. And the pH has a significant effect on the response than the MIPs dosage. The removal effect is best when the pH is 5–6 at constant MIPs dosage.

### 3.2.4. Prediction and verification of optimal conditions

To support the optimized data given by numerical modeling under optimized conditions, the confirmatory

Table 4  
Optimal process conditions for 4-NP removal by MIPs

4-NP concentration ( $\mu\text{mol/L}$ )	MIPs dosage (g/L)	Temperature (K)	pH	Removal rate of 4-NP, $E$ (%)	
				Predicted	Experimental
10	1.46	294.2	5.6	79.63	78.39

Table 5  
Comparison of the adsorption capacity MIPs with some previously reported adsorbents for 4-NP

Adsorbent	$q_{\text{max}}$ (mg/g)	References
Calix[6]arene-tethered silica	2.3	[43]
CD-MIP	26.87	[44]
Methacryloyl antipyrine/ 4-nitrophenol-MIPs	25.9	[45]
Pure graphene	15.5	[46]
Metal-organic framework (Cr-BDC)	19.0	[47]
Activated carbon from peach stones and treated with urea	234	[48]
PVA-L-arginine membrane	6.78	[49]
Silver(I) 3,5-diphenyltriazolate MOF	48.4	[50]
MIPs (This study)	15.09	This study

experiments were conducted with the parameters as suggested by the model. As shown in Table 4, the optimum operating condition is found at the initial concentration of 4-NP 10  $\mu\text{mol/L}$ , the MIPs dosage 1.46 g/L, the solution temperature 294.2 K and the solution pH 5.60, and optimal removal efficiency of 4-NP was found to be 79.63%. According to the optimal parameters, three sets of parallel adsorption experiments were performed, and the 4-NP removal rate was finally obtained at 78.39%, which was practically in agreement with the results obtained from the optimization of numerical modeling. The results proved the accuracy and reliability of the regression model is suitable for 4-NP removal by MIPs.

### 3.3. Comparison with other adsorbents for Cr(VI)

To objectively evaluate the ability of the prepared MIPs to remove 4-NP, we here compared the maximum adsorption capacity ( $q_{\text{max}}$ ) in our study with those of other recent publications. The results are listed in Table 5, we summarized 9 studies with diverse types of the adsorbent for 4-NP, including polymer compositions and carbon materials. In the category of selective adsorption, the prepared MIPs exhibited comparable adsorption capacity within a relatively short time. The adsorption capacity was also relatively high among the non-selective adsorbents. However, activated carbon and Metal-organic Framework exhibited the best adsorption capacity, which was due to the large surface areas of these materials.

## 4. Conclusion

In the current work, we prepared a novel imprinted material (MIPs) by using surface Molecular Imprinting Technology combined with the sol-gel method. 4-level Box-Behnken design (BBD) in response surface methodology (RSM) was used to optimize the process parameters of the removal of 4-NP adsorbed on MIPs, viz., initial concentration of 4-NP, MIPs dosage, solution pH, and temperature. The results of analysis of variance (ANOVA) test revealed that the effect of all parameters on the removal efficiency of the 4-NP was significant (Prob.  $> F < 0.05$ ), except initial concentration, interaction between pH and temperature, and interaction between pH and initial concentration. The highest 4-NP removal efficiency (78.39%) can be achieved at the optimal conditions of initial 4-NP concentration, MIPs dosage, temperature, and pH of 10  $\mu\text{mol/L}$ , 1.46 g/L, 294.2 K, and 5.60, respectively, which close to the predicted value (79.63%) under the same conditions. The theoretical model constructed by RSM can be used to optimize the adsorption conditions of 4-NP in water, while other optimization scenarios can be suggested to give the maximum removal of 4-NP based on the available resources. As a result, the findings in this paper indicated that MIPs could be used as an efficient and novel adsorbent for the removal of 4-NP.

## Acknowledgements

The authors acknowledged the financial support of the State Key Laboratory of Urban Water Resource and Environment (Harbin Institute of Technology) (No. ES201917), Key project of natural science foundation of Anhui provincial department of education (No. KJ2019A0056), and natural science foundation youth program of Anhui (No. 2008085QE242), the project of cultivating top talents for the universities in Anhui Province (Grant No. gxyqZD2017036).

## Declaration of interests

The authors declare that they have no known competing financial interests or personal relationships that could have appeared to influence the work reported in this paper.

## Data availability statement

All relevant data are included in the paper or its Supplementary Information.

## References

- [1] Y. Choi, M.-J. Choi, S.-H. Cha, Y.S. Kim, S. Cho, Y. Park, Catechin-capped gold nanoparticles: green synthesis, characterization,

- and catalytic activity toward 4-nitrophenol reduction, *Nanoscale Res. Lett.*, 9 (2014) 103, doi: 10.1186/1556-276X-9-103.
- [2] M.I. Din, R. Khalid, Z. Hussain, T. Hussain, A. Mujahid, J. Najeeb, F. Izhar, Nanocatalytic assemblies for catalytic reduction of nitrophenols: a critical review, *Crit. Rev. Anal. Chem.*, 50 (2020) 322–338.
- [3] M. Ramalingam, V.K. Ponnusamy, S.N. Sangilimuthu, Electrochemical determination of 4-nitrophenol in environmental water samples using porous graphitic carbon nitride-coated screen-printed electrode, *Environ. Sci. Pollut. Res.*, 27 (2020) 17481–17491.
- [4] M. Liu, Z. Gao, Y. Yu, R. Su, R. Huang, W. Qi, Z. He, Molecularly imprinted core-shell CdSe@SiO<sub>2</sub>/CDs as a ratiometric fluorescent probe for 4-nitrophenol sensing, *Nanoscale Res. Lett.*, 13 (2018) 27, doi: 10.1186/s11671-018-2440-6.
- [5] N. Belachew, R. Fekadu, A. Ayalew Abebe, RSM-BBD optimization of fenton-like degradation of 4-nitrophenol using magnetite impregnated kaolin, *Air Soil Water Res.*, 13 (2020) 117862212093212, doi: 10.1177/1178622120932124.
- [6] I. Ivančev-Tumbas, R. Hobby, B. Küchle, S. Panglisch, R. Gimbel, p-Nitrophenol removal by combination of powdered activated carbon adsorption and ultrafiltration – comparison of different operational modes, *Water Res.*, 42 (2008) 4117–4124.
- [7] S.Y. Rodríguez, M.E. Cantú, B. Garcia-Reyes, M.T. Garza-Gonzalez, E.R. Meza-Escalante, D. Serrano, L.H. Alvarez, Biotransformation of 4-nitrophenol by co-immobilized *Geobacter sulfurreducens* and anthraquinone-2-sulfonate in barium alginate beads, *Chemosphere*, 221 (2019) 219–225.
- [8] A.A. Werkneh, S.B. Gebru, G.H. Redae, A.G. Tsige, Removal of endocrine disruptors from the contaminated environment: public health concerns, treatment strategies and future perspectives – a review, *Heliyon*, 8 (2022) e09206.
- [9] M.J. Whitcombe, N. Kirsch, I.A. Nicholls, Molecular imprinting science and technology: a survey of the literature for the years 2004–2011, *J. Mol. Recognit.*, 27 (2014) 297–401.
- [10] D.-L. Huang, R.-Z. Wang, Y.-G. Liu, G.-M. Zeng, C. Lai, P. Xu, B.-A. Lu, J.-J. Xu, C. Wang, C. Huang, Application of molecularly imprinted polymers in wastewater treatment: a review, *Environ. Sci. Pollut. Res.*, 22 (2015) 963–977.
- [11] T. Li, L. Fan, Y. Wang, X. Huang, J. Xu, J. Lu, M. Zhang, W. Xu, Molecularly imprinted membrane electrospray ionization for direct sample analyses, *Anal. Chem.*, 89 (2017) 1453–1458.
- [12] Y. Huang, Y. Xu, Q. He, B. Du, Y. Cao, Preparation and characteristics of a dummy molecularly imprinted polymer for phenol, *J. Appl. Polym. Sci.*, 128 (2013) 3256–3262.
- [13] A. Yigaimu, T. Muhammad, W. Yang, I. Muhammad, M. Wubulikasimu, S.A. Piletsky, Magnetic molecularly imprinted polymer particles based micro-solid phase extraction for the determination of 4-nitrophenol in lake water, *Macromol. Res.*, 27 (2019) 1089–1094.
- [14] L. Li, F. Zhu, Y. Lu, J. Guan, Synthesis, adsorption and selectivity of inverse emulsion Cd(II) imprinted polymers, *Chin. J. Chem. Eng.*, 26 (2018) 494–500.
- [15] W. Zhang, Q. Li, J. Cong, B. Wei, S. Wang, Mechanism analysis of selective adsorption and specific recognition by molecularly imprinted polymers of ginsenoside Re, *Polymers*, 10 (2018) 216, doi: 10.3390/polym10020216.
- [16] F. Zhu, Y. Lu, T. Ren, S. He, Y. Gao, Synthesis of ureido-functionalized Cr(VI) imprinted polymer: adsorption kinetics and thermodynamics studies, *Desal. Water Treat.*, 100 (2017) 126–134.
- [17] C. Dong, H. Shi, Y. Han, Y. Yang, R. Wang, J. Men, Molecularly imprinted polymers by the surface imprinting technique, *Eur. Polym. J.*, 145 (2021) 110231, doi: 10.1016/j.eurpolymj.2020.110231.
- [18] M.P. Di Bello, L. Mergola, S. Scorrano, R. Del Sole, Towards a new strategy of a chitosan-based molecularly imprinted membrane for removal of 4-nitrophenol in real water samples: chitosan-based molecularly imprinted membranes, *Polym. Int.*, 66 (2017) 1055–1063.
- [19] F.-Q. An, H.-F. Li, X.-D. Guo, T.-P. Hu, B.-J. Gao, J.-F. Gao, Design of novel “imprinting synchronized with crosslinking” surface imprinted technique and its application for selectively removing phenols from aqueous solution, *Eur. Polym. J.*, 112 (2019) 273–282.
- [20] W. Liang, Y. Lu, N. Li, H. Li, F. Zhu, Microwave-assisted synthesis of magnetic surface molecular imprinted polymer for adsorption and solid phase extraction of 4-nitrophenol in wastewater, *Microchem. J.*, 159 (2020) 105316, doi: 10.1016/j.microc.2020.105316.
- [21] Y. Li, H.-H. Yang, Q.-H. You, Z.-X. Zhuang, X.-R. Wang, Protein recognition via surface molecularly imprinted polymer nanowires, *Anal. Chem.*, 78 (2006) 317–320.
- [22] C.A. Mourão, F. Bokeloh, J. Xu, E. Prost, L. Duma, F. Merlier, S.M.A. Bueno, K. Haupt, B. Tse Sum Bui, Dual-oriented solid-phase molecular imprinting: toward selective artificial receptors for recognition of nucleotides in water, *Macromolecules*, 50 (2017) 7484–7490.
- [23] K. Phonklam, R. Wannapob, W. Sriwimol, P. Thavarungkul, T. Phairatana, A novel molecularly imprinted polymer PMB/MWCNTs sensor for highly-sensitive cardiac troponin T detection, *Sens. Actuators, B*, 308 (2020) 127630, doi: 10.1016/j.snb.2019.127630.
- [24] A. Mehdinia, S. Dadkhah, T. Baradaran Kayyal, A. Jabbari, Design of a surface-immobilized 4-nitrophenol molecularly imprinted polymer via pre-grafting amino functional materials on magnetic nanoparticles, *J. Chromatogr. A*, 1364 (2014) 12–19.
- [25] L. Wang, K. Zhi, Y. Zhang, Y. Liu, L. Zhang, A. Yasin, Q. Lin, Molecularly imprinted polymers for gossypol via sol–gel, bulk, and surface layer imprinting—a comparative study, *Polymers*, 11 (2019) 602, doi: 10.3390/polym11040602.
- [26] M.M. Moein, A. Abdel-Rehim, M. Abdel-Rehim, Recent applications of molecularly imprinted sol–gel methodology in sample preparation, *Molecules*, 24 (2019) 2889, doi: 10.3390/molecules24162889.
- [27] L. Guo, X. Ma, X. Xie, R. Huang, M. Zhang, J. Li, G. Zeng, Y. Fan, Preparation of dual-dummy-template molecularly imprinted polymers coated magnetic graphene oxide for separation and enrichment of phthalate esters in water, *Chem. Eng. J.*, 361 (2019) 245–255.
- [28] T. Hao, X. Wei, Y. Nie, Y. Xu, Y. Yan, Z. Zhou, An eco-friendly molecularly imprinted fluorescence composite material based on carbon dots for fluorescent detection of 4-nitrophenol, *Microchim. Acta*, 183 (2016) 2197–2203.
- [29] S. Raof, S. Mohamad, M. Abas, Synthesis and evaluation of molecularly imprinted silica gel for 2-hydroxybenzoic acid in aqueous solution, *Int. J. Mol. Sci.*, 14 (2013) 5952–5965.
- [30] G. Xue, L. Ding, Y. Gao, M. Zhong, Preparation and properties characterization of 4-nitrophenol imprinted materials by surface imprinting coupled with sol–gel method, *Chin. J. Process Eng.*, 20 (2020) 440–448 (in Chinese).
- [31] G. Xie, R. Li, Y. Han, Y. Zhu, G. Wu, M. Qin, Optimization of the extraction conditions for *Buddleja officinalis maxim*. Using response surface methodology and exploration of the optimum harvest time, *Molecules*, 22 (2017) 1877, doi: 10.3390/molecules22111877.
- [32] A. Azari, M. Yeganeh, M. Gholami, M. Salari, The superior adsorption capacity of 2,4-dinitrophenol under ultrasound-assisted magnetic adsorption system: modeling and process optimization by central composite design, *J. Hazard. Mater.*, 418 (2021) 126348, doi: 10.1016/j.jhazmat.2021.126348.
- [33] M.Y. Badi, A. Esrafil, H. Pasalari, R.R. Kalantary, E. Ahmadi, M. Gholami, A. Azari, Degradation of dimethyl phthalate using persulfate activated by UV and ferrous ions: optimizing operational parameters mechanism and pathway, *J. Environ. Health Sci. Eng.*, 17 (2019) 685–700.
- [34] V. Alimohammadi, M. Sedighi, E. Jabbari, Optimization of sulfate removal from wastewater using magnetic multi-walled carbon nanotubes by response surface methodology, *Water Sci. Technol.*, 76 (2017) 2593–2602.
- [35] A.S. Abdulhameed, A.-T. Mohammad, A.H. Jawad, Application of response surface methodology for enhanced synthesis of chitosan triphosphate/TiO<sub>2</sub> nanocomposite and adsorption of reactive orange 16 dye, *J. Cleaner Prod.*, 232 (2019) 43–56.
- [36] A. Poudel, M.A. Fernandez, S.A.M. Tofail, M.J.P. Biggs, Boron nitride nanotube addition enhances the crystallinity and

- cytocompatibility of PVDF-TrFE, *Front. Chem.*, 7 (2019) 364, doi: 10.3389/fchem.2019.00364.
- [37] J. Pan, X. Zou, X. Wang, W. Guan, Y. Yan, J. Han, Selective recognition of 2,4-dichlorophenol from aqueous solution by uniformly sized molecularly imprinted microspheres with  $\beta$ -cyclodextrin/attapulgitite composites as support, *Chem. Eng. J.*, 162 (2010) 910–918.
- [38] F.S. Moosavi, T. Tavakoli, Amoxicillin degradation from contaminated water by solar photocatalysis using response surface methodology (RSM), *Environ. Sci. Pollut. Res.*, 23 (2016) 23262–23270.
- [39] Y. Zhang, Z. Tian, Q. Jing, Y. Chen, X. Huang, Removal of Cr(VI) by modified diatomite supported NZVI from aqueous solution: evaluating the effects of removal factors by RSM and understanding the effects of pH, *Water Sci. Technol.*, 80 (2019) 308–316.
- [40] X. Zhang, X. Lu, S. Li, M. Zhong, X. Shi, G. Luo, L. Ding, Investigation of 2,4-dichlorophenoxyacetic acid adsorption onto MIEX resin: optimization using response surface methodology, *J. Taiwan Inst. Chem. Eng.*, 45 (2014) 1835–1841.
- [41] M. Mourabet, A. El Rhilassi, H. El Boujaady, M. Bennani-Ziatni, A. Taitai, Use of response surface methodology for optimization of fluoride adsorption in an aqueous solution by brushite, *Arabian J. Chem.*, 10 (2017) S3292–S3302.
- [42] N. Jadbabaei, R.J. Slobodjian, D. Shuai, H. Zhang, Catalytic reduction of 4-nitrophenol by palladium-resin composites, *Appl. Catal., A*, 543 (2017) 209–217.
- [43] M. Dogan, F. Temel, M. Tabakci, High-performance adsorption of 4-nitrophenol onto calix[6]arene-tethered silica from aqueous solutions, *J. Inorg. Organomet. Polym. Mater.*, 30 (2020) 4191–4202.
- [44] D. Lang, M. Shi, X. Xu, S. He, C. Yang, L. Wang, R. Wu, W. Wang, J. Wang, DMAEMA-grafted cellulose as an imprinted adsorbent for the selective adsorption of 4-nitrophenol, *Cellulose*, 28 (2021) 6481–6498.
- [45] R. Say, A. Ersöz, İ. Şener, A. Atılır, S. Diltemiz, A. Denizli, Comparison of adsorption and selectivity characteristics for 4-nitrophenol imprinted polymers prepared via bulk and suspension polymerization, *Sep. Sci. Technol.*, 39 (2005) 3471–3484.
- [46] A.I. Ismail, Thermodynamic and kinetic properties of the adsorption of 4-nitrophenol on graphene from aqueous solution, *Can. J. Chem.*, 93 (2015) 1083–1087.
- [47] J. Chen, X. Sun, L. Lin, X. Dong, Y. He, Adsorption removal of o-nitrophenol and p-nitrophenol from wastewater by metal-organic framework Cr-BDC, *Chin. J. Chem. Eng.*, 25 (2017) 775–781.
- [48] S. Álvarez-Torrellas, M. Martín-Martínez, H.T. Gomes, G. Ovejero, J. García, Enhancement of p-nitrophenol adsorption capacity through  $N_2$ -thermal-based treatment of activated carbons, *Appl. Surf. Sci.*, 414 (2017) 424–434.
- [49] T. Narkkun, P. Boonying, C. Yuenyao, S. Amnuaypanich, Green synthesis of porous polyvinyl alcohol membranes functionalized with l-arginine and their application in the removal of 4-nitrophenol from aqueous solution, *J. Appl. Polym. Sci.*, 136 (2019) 47835, doi: 10.1002/app.47835.
- [50] H. Miao, S. Song, H. Chen, W. Zhang, R. Han, G. Yang, Adsorption study of p-nitrophenol on a silver(I) triazolate MOF, *J. Porous Mater.*, 27 (2020) 1409–1417.